

Rolling Circle Amplification-Templated DNA Nanotubes Show Increased Stability and Cell Penetration Ability

Graham D. Hamblin, Karina M. M. Carneiro, Johans F. Fakhoury, Katherine E. Bujold, and Hanadi F. Sleiman*

Department of Chemistry, McGill University, 801 Sherbrooke Street West, Montreal, QC H3A 2K6 Canada

S Supporting Information

ABSTRACT: DNA nanotubes hold promise as scaffolds for protein organization, as templates of nanowires and photonic systems, and as drug delivery vehicles. We present a new DNA-economic strategy for the construction of DNA nanotubes with a backbone produced by rolling circle amplification (RCA), which results in increased stability and templated length. These nanotubes are more resistant to nuclease degradation, capable of entering human cervical cancer (HeLa) cells with significantly increased uptake over double-stranded DNA, and are amenable to encapsulation and release behavior. As such, they represent a potentially unique platform for the development of cell probes, drug delivery, and imaging tools.

Well-defined nanoscale building blocks have become increasingly attractive in current technologies such as nanoelectronics, biomedical engineering, drug delivery, and nanorobotics.¹ While current nanoobjects tend to be built from many separate building blocks, nature often relies on processive cycles to produce highly complex machinery from a template, as with protein biosynthesis. This allows the production of intricate, precise structures from simple starting materials via a single assembly pathway.

DNA has recently emerged as a versatile material for nanoscale construction, resulting in a wide variety of well-defined and functional objects.^{2,3} Because of its highly predictable Watson–Crick base-pairing behavior, structural definition, and ease of synthesis, it is an ideal molecule for self-assembly. A distinct advantage of DNA as a biological molecule is its ability to be used as a template in cellular processes. As such, it should be amenable to construction strategies that draw on biological mechanisms. Indeed, several groups have reported the use of polymerases, ligases, and even bacteria to produce DNA nanostructures enzymatically or augment their properties.^{4–6} Work has also progressed in using DNA structures for cellular delivery, through its intrinsic recognition capabilities,⁷ nonspecific uptake,^{8,9} and via functionalization with targeting groups.¹⁰ This communication describes the use of rolling circle amplification (RCA) in producing well-defined DNA nanotubes that possess increased nuclease resistance, can enter cells significantly more efficiently than double-stranded DNA, and as such are promising for potential applications in drug delivery.

We have previously reported the design and synthesis of modular DNA nanotubes with controlled shape, length, and rigidity^{11,12} that are capable of encapsulation and subsequent release of cargo.¹³ They are composed of small geometric “rungs”, set within vertical tracks of duplex DNA (“struts”). The rung is built on a closed triangular strand, with synthetic insertions at each vertex to provide orientation and rigidity (see Figure 1b, inset). Materials with a high aspect ratio are known to elicit unique responses in biological systems relative to spherical objects, such as increased membrane penetration and cellular internalization,^{14–16} and decreased uptake by phagocytic cells resulting in longer circulation times.¹⁷ Dense DNA structures have also been shown to be more resistant to degradation by nucleases¹⁸ and possess improved cellular uptake properties.¹⁹ Thus, a high aspect ratio DNA nanotube for which encapsulation and release have already been demonstrated could have unique potential as a drug delivery vehicle.

In this work, we use a synthetic design that yields robust, structurally uniform DNA nanotubes, capable of resisting nuclease degradation and entering HeLa cells. Nicks (i.e., points where the phosphodiester DNA backbone is broken) along the struts of nanotube designs are likely weak points, providing handles for exonuclease activity and promoting disassembly into smaller structures. As such, reducing the number of nicks would increase nanotube stability, a hypothesis that was supported by the success of Fyngenson and co-workers⁶ in stabilizing tile-based DNA nanotubes through ligation.

Rolling circle amplification (RCA) is an enzymatic process that produces long, single-stranded DNA of periodic sequence from a cyclic template. It has been used to organize long tracks of proteins²⁰ and nanoparticles.²¹ RCA from a ligated template was used to create a continuous, non-nicked backbone strand RCA (~1400–15000 bases long) that replaces one of the struts and guides nanotube assembly, as outlined in Figure 1. The RCA product has two distinct, alternating sequences (Figure 1a): a binding region (BR) for attaching rungs and an intervening spacer region (SR, complementary to spacer strand 1a). Rung 2 was constructed from a triangular strand (T) containing synthetic triaryl vertices, as reported previously,¹¹ and was designed with a complementary binding region BR'. This was assembled separately in quantitative yield with a 3.5 h thermal anneal from 95 to 4 °C (Figure 1b). Combining these products gave a long, open-form nanotube with a continuous

Received: November 15, 2011

Published: January 26, 2012

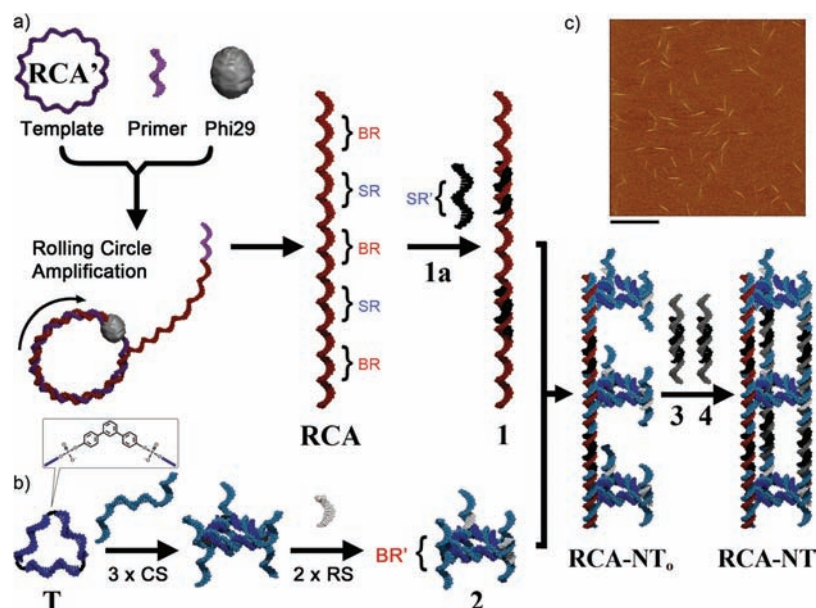


Figure 1. RCA nanotube design. (a) A cyclic template is combined with a primer strand and DNA polymerase Phi29, producing long, periodic single-stranded DNA RCA. This has alternating binding (BR) and spacer (SR) regions and can be hybridized to spacer strand 1a (with complementary sequence SR') to form 1. (b) Triangular rung 2 is prepared in a stepwise manner from a closed triangle, three complementary strands with overhangs at each end (CS), and two rigidifying strands to orient the overhangs (RS). See Supporting Information for characterization of these processes. (c) Combining the two products yields an open form nanotube RCA-NT₀, which can be closed to the full nanotube RCA-NT with the addition of double-stranded linkers 3 and 4. AFM characterization confirms the presence of RCA-NT (phase image, scale bar is 2.5 μm). Note that only 3 repeats are shown for clarity; each nanotube has 25–250 rungs in reality.

backbone (RCA-NT₀). Subsequent addition of double-stranded linkers 3–4 formed the remaining struts, giving a fully double-stranded triangular nanotube (RCA-NT).²² Atomic force microscopy (AFM) characterization confirmed the successful preparation of RCA-NT (Figure 1c). When dried on an HOPG surface, the tubes appear to be quite rigid and exist in either single tubes or small bundles of $0.71 \pm 0.17 \mu\text{m}$ in length, while higher concentration samples are more bundled (Supporting Information). This length correlates well with the estimated length of RCA ($0.85 \pm 1.51 \mu\text{m}$) and is different than observed for our original nanotube design (NT) under equivalent conditions ($1.2 \pm 0.5 \mu\text{m}$).²² Further, when a longer $\sim 12 \mu\text{m}$ RCA fraction was isolated and used for nanotube preparation, nanotubes of $10.2 \pm 3.9 \mu\text{m}$ in length were observed instead.²² Together, this confirms that the RCA backbone templates and plays a role in defining the length of the nanotubes.

To explore the stability of RCA-NT in serum, a degradation assay was performed in 10% fetal bovine serum (FBS)/PBS over 22 h. As can be seen from Figure 2, RCA-NT exhibits increased nuclease resistance as compared to both double-stranded DNA (dsDNA) and NT. Samples were denatured after exposure and analyzed by polyacrylamide gel electrophoresis (PAGE), yielding a fingerprint band pattern of component strands that could be tracked across time points. Total band intensity was obtained with ImageJ, charted for each sample, and the first-order decay rates were determined (Figure 2b). With a half-life of 2.5 h, RCA-NT is roughly five times more stable than double-stranded DNA and three times more stable than NT in serum.

Finally, we examined the ability of RCA-NT to cross the plasma membrane and enter cells. Single- or double-stranded DNA typically shows limited cell permeability, requiring the use of transfection agents (viruses, cationic polymers, etc.) for

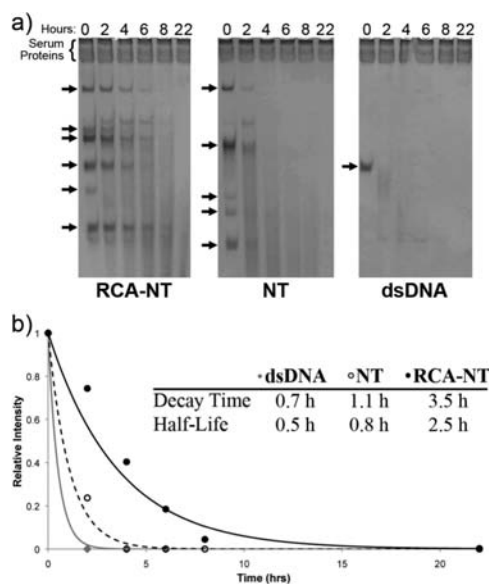


Figure 2. Serum stability assay. (a) Denaturing PAGE analysis of RCA-NT, NT, and double-stranded DNA control dsDNA after varied exposure times with 10% FBS. Arrows mark the bands used for analysis in each case. (b) Fitted data. All three samples followed first-order decay, with equations as indicated. The corresponding half-lives are also given.

efficient cell entry. However, the dense display of DNA and high aspect ratio of RCA-NT can possibly allow their enhanced cellular penetration over normal DNA. For imaging, one RS strand was labeled at the 5' end with either a Cy5 or Cy3 fluorophore, resulting in labeled triangular rungs. We verified that the incorporation of these dyes into the nanotube was quantitative, and these modifications did not affect the

assembly of either rung or nanotube.²² Upon incubation of HeLa cells with a Cy3, Cy5, or mixed population nanotube (i.e., both fluorophores on any given nanotube) for 6 h, cells exhibited a significant fluorescence intensity for the appropriate fluorophore as determined by fluorescence-activated cell sorting (FACS). Confocal microscopy confirmed that the dyes were inside the cells, rather than adhered to the surface, and that Cy3 and Cy5 were colocalized in the mixed population sample. This suggests that the nanotube enters as a cohesive unit (as intact or partially intact nanotube), rather than breaking down to its components, which would have no reason to colocalize. In contrast, Cy3-labeled dsDNA gave negligible uptake, as outlined in Figure 3.

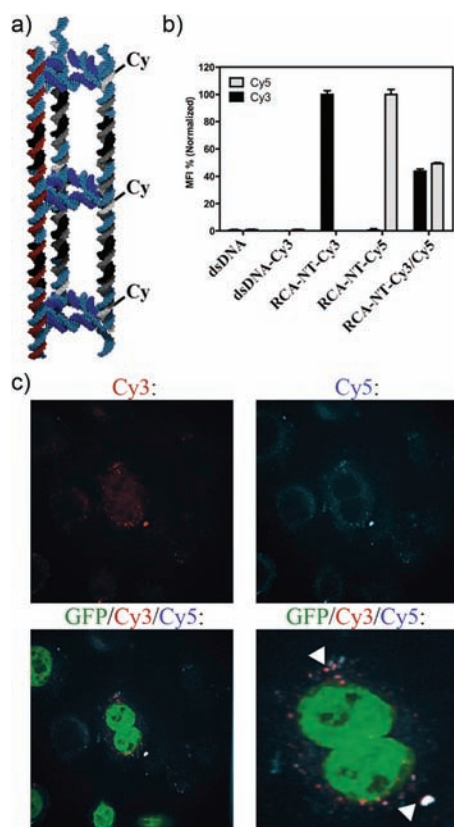


Figure 3. Cellular uptake of RCA-NT. (a) The nanotube is labeled with a Cy3 or Cy5 fluorophore at the 5' end of one of its RS strands. (b) FACS data for Cy3-, Cy5-, and mixed label RCA-NT and Cy3-labeled duplex DNA. Cells were incubated with DNA for 4 h, then adjusted to 30% FBS, and incubated for 2 more hours. After fixation and sorting, the normalized mean fluorescence intensity was determined for each sample. (c) Confocal microscopy images of mixed Cy3/Cy5 nanotubes, demonstrating colocalization of the fluorophores inside HeLa cells. White arrows indicate examples of colocalized signals.

Previously, Mao and colleagues¹⁰ have reported folate-mediated uptake of DNA nanotubes (in their entirety or as fragments), and Turberfield's group⁸ has demonstrated moderate uptake of a tetrahedral structure. Interestingly, we observe highly enhanced cellular penetration over that of duplex DNA, without the need for transfection agents or targeting groups. These studies parallel those of the Mirkin group, which show that a dense arrangement of a shell of DNA strands in core-shell structures can also result in efficient cell uptake without the need for transfection.²³ Recent studies have

identified the anionic ligand-binding receptor (ALBR) pathway⁹ or uptake mediated by scavenger receptors²⁴ as possibly relevant to cellular internalization of unlabeled dense DNA structures. The mechanism involved here is currently under exploration.

In conclusion, we have reported a novel, simplified, and DNA-economic approach to build robust DNA nanotubes that are resistant to nuclease degradation. This is based on the use of rolling circle amplification to produce a long template strand onto which DNA nanotubes can be built. In addition, we show more efficient uptake of an unlabeled DNA nanostructure than any previous report. We demonstrate the integrity of our nanostructures as they are internalized in cells. The resulting products present a clear step forward over previous nanotube designs, requiring a small number of starting DNA strands, and demonstrating templated length and increased nuclease stability. RCA nanotubes should retain the encapsulation and release properties that we have already established.¹³ With multiple addressable and repeating sites, these nanotubes should also be compatible with labeling for targeted uptake, decreased immune response, or further protection against degradation. Together, this gives them promising potential for applications as cellular probes as well as drug delivery and imaging tools.

■ ASSOCIATED CONTENT

📄 Supporting Information

Experimental details, DNA sequences, characterization of individual components, AFM and cellular uptake control experiments. This material is available free of charge via the Internet at <http://pubs.acs.org>.

■ AUTHOR INFORMATION

Corresponding Author

hanadi.sleiman@mcgill.ca

Notes

The authors declare no competing financial interest.

■ ACKNOWLEDGMENTS

We thank NSERC, CFI, CSACS, and CIFAR. H.F.S. is a Cottrell Scholar of the Research Corporation.

■ REFERENCES

- (1) Cao, G. *Nanostructures and Nanomaterials - Synthesis, Properties and Applications*; Imperial College: London, 2004; p 110.
- (2) Aldaye, F. A.; Palmer, A. L.; Sleiman, H. F. *Science* **2008**, *321*, 1795–1799.
- (3) Lin, C.; Liu, Y.; Yan, H. *Biochemistry* **2009**, *48*, 1663–1674.
- (4) Goodman, R. P.; Schapp, I. A. T.; Tardin, C. F.; Erben, C. M.; Berry, R. M.; Schmidt, C. F.; Turberfield, A. J. *Science* **2005**, *310*, 1661–1665.
- (5) Lin, C.; Rinker, S.; Wang, X.; Liu, Y.; Seeman, N. C.; Yan, H. *Proc. Natl. Acad. Sci. U.S.A.* **2008**, *105*, 17626–17631.
- (6) O'Neill, P.; Rothmund, P. W. K.; Kumar, A.; Fygenson, D. K. *Nano Lett.* **2006**, *6*, 1379–1383.
- (7) Chang, M.; Yang, C.-S.; Huang, D.-M. *ACS Nano* **2011**, *5*, 6156–6163.
- (8) Walsh, A. S.; Yin, H.; Erben, C. M.; Wood, M. J. A.; Turberfield, A. J. *ACS Nano* **2011**, *5*, 5427–5432.
- (9) Bhatia, D.; Surana, S.; Chakraborty, S.; Koushika, S. P.; Krishnan, Y. *Nat. Commun.* **2011**, *2*, 339.
- (10) Ko, S.; Liu, H.; Chen, Y.; Mao, C. *Biomacromolecules* **2008**, *9*, 3039–3043.

- (11) Aldaye, F. A.; Lo, P. K.; Karam, P.; McLaughlin, C. K.; Cosa, G.; Sleiman, H. F. *Nat. Nanotechnol.* **2009**, *4*, 349–352.
- (12) Lo, P. K.; Altvater, F.; Sleiman, H. F. *J. Am. Chem. Soc.* **2010**, *132*, 10212–10214.
- (13) Lo, P. K.; Karam, P.; Aldaye, F. A.; McLaughlin, C. K.; Hamblin, G. D.; Cosa, G.; Sleiman, H. F. *Nat. Chem.* **2010**, *2*, 319–328.
- (14) Zhang, Y.; Ali, S. F.; Dervishi, E.; Xu, Y.; Li, Z.; Casciano, D.; Biris, A. S. *ACS Nano* **2010**, *4*, 3181–3186.
- (15) Gratton, S. E. A.; Ropp, P. A.; Pohlhaus, P. D.; Luft, J. C.; Madden, V. J.; Napier, M. E.; DeSimone, J. M. *Proc. Natl. Acad. Sci. U.S.A.* **2008**, *105*, 11613–11618.
- (16) Alemdaroglu, F. E.; Alemdaroglu, N. C.; Langguth, P.; Herrmann, A. *Macromol. Rapid Commun.* **2008**, *29*, 326–329.
- (17) Longmire, M. R.; Ogawa, M.; Choyke, P. L.; Kobayashi, H. *Bioconjugate Chem.* **2011**, *22*, 993–1000.
- (18) Keum, J.-W.; Bermudez, H. *Chem. Commun.* **2009**, 7036–7038.
- (19) Cutler, J. I.; Zhang, K.; Zheng, D.; Auyeung, E.; Prigodich, A. E.; Mirkin, C. A. *J. Am. Chem. Soc.* **2011**, *133*, 9254–9257.
- (20) Beyer, S.; Nickels, P.; Simmel, F. C. *Nano Lett.* **2005**, *5*, 719–722.
- (21) Deng, Z.; Tian, Y.; Lee, S.-H.; Ribbe, A. E.; Mao, C. *Angew. Chem., Int. Ed.* **2005**, *44*, 3582–3585.
- (22) See Supporting Information for additional experimental details.
- (23) Giljohann, D. A.; Seferos, D. S.; Patel, P. C.; Millstone, J. E.; Rosi, N. L.; Mirkin, C. A. *Nano Lett.* **2007**, *7*, 3818–3821.
- (24) Patel, P. C.; Giljohann, D. A.; Daniel, W. L.; Zheng, D.; Prigodich, A. E.; Mirkin, C. A. *Bioconjugate Chem.* **2010**, *21*, 2250–2256.